

## Cluster-phonon model applied to the $^{91}\text{Zr}$ nucleus

L. Losano and M. de O. Roos

*Departamento de Física, Universidade Federal da Paraíba, C.P. 5008, 58059 João Pessoa, PB, Brasil*

H. Dias

*Instituto de Física, Universidade de São Paulo, C.P. 20516, 01498 São Paulo, SP, Brasil*

(Received 3 June 1992)

The structure of the low-lying levels of the  $^{91}\text{Zr}$  nucleus is discussed in a framework of the cluster-phonon coupling model. In order to describe simultaneously positive- and negative-parity states, octupole as well as quadrupole vibrations of the  $^{88}\text{Sr}$  core are allowed. The cluster states include two single protons coupled to a single neutron. The residual interaction among the cluster particles is assumed to be the modified surface  $\delta$  interaction. Energy levels and electromagnetic properties are calculated and compared with the experimental data.

PACS number(s): 21.60.Gx, 27.60.+j

### I. INTRODUCTION

Previous calculations of the low-lying level characteristics of  $^{91}\text{Zr}$  have relied, with few exceptions, on increasingly elaborate shell-model schemes. The first calculations by Talmi [1] considered only  $(d_{5/2})^n$  configurations and were aimed at reconstructing the spectrum of levels. More recent calculations [2–4] consider the  $p_{1/2}$  and  $g_{9/2}$  orbitals for the protons and  $d_{5/2}$  and  $s_{1/2}$  for the neutrons. In addition, Chuu *et al.* [4] include the  $d_{3/2}$  and  $g_{7/2}$  neutron orbitals, and Ipson *et al.* [3] consider the  $h_{11/2}$  neutron orbital. These works studied the spectrum of levels, spectroscopic factors for one-particle pickup and stripping, and, in a few cases, transition probabilities [2–5].

In our earlier work [6], the lifetimes of the low-lying positive-parity levels were measured by the Doppler shift attenuation method and calculated using the model of Chuu *et al.* [4]. The values of effective charges needed to adjust the experimental results suggest a reasonable core polarization. Earlier evidences from electron scattering [7,8] have indicated that the charge and current densities for  $E5$  [7] and  $E2$  [8] transitions can only originate from  $^{88}\text{Sr}$  core excitations.

In the case of  $N=50$  isotones, for those nuclei dominated by excitations in proton ( $p_{1/2}, g_{9/2}$ ) space, standard shell-model calculations have been quite successful in reproducing energy levels and many other nuclear properties. However, in the  $^{90}\text{Zr}$  nucleus, most of the low-lying negative-parity states and a few odd angular momentum positive-parity states cannot be explained with this model.

Recently, the  $^{88}\text{Sr}$  core excitations were included by Ji and Wildenthal [9] by means of an extended shell model in a proton ( $f_{5/2}, p_{3/2}, p_{1/2}, g_{9/2}$ ) space. They obtain an excellent reproduction of the  $^{88}\text{Sr}$  levels and many of the measured energy levels, in  $N=50$  isotones, are well fitted. In particular, for the  $^{90}\text{Zr}$  nuclide, predicted excitation energies for states with spins up to  $11^+$  and  $11^-$  are in

good agreement with experimental data, up to about 7 MeV.

The inclusion of the proton  $f_{5/2}$  and  $p_{3/2}$  orbitals, as in the  $^{99}\text{Zr}$  nucleus, is quite difficult in  $^{91}\text{Zr}$  due to the dimension of the matrices. In this case, a semimicroscopic description (cluster-phonon coupling model) is a very good starting point for theoretical studies.

In the past few years, the cluster-phonon model was employed for nuclei with  $A \approx 90$  ( $^{88}\text{Y}$ ,  $^{89}\text{Y}$ ,  $^{90}\text{Y}$ ,  $^{87}\text{Sr}$ , and  $^{89}\text{Sr}$ ) to describe simultaneously positive- and negative-parity states, in which quadrupole as well as octupole vibrations of the  $^{88}\text{Sr}$  core are allowed [10,11]. These calculations provided a reasonably good fit to observed level energies, spectroscopic factors, and some electromagnetic properties, showing that the general trend of experimental data in this mass region can be interpreted within the cited model. Therefore, we extend the cluster-(quadrupole-octupole) phonon model, including two protons, and one neutron in the cluster, to explain the nuclear structure of low-lying positive- and negative-parity states in  $^{91}\text{Zr}$ . The more recent theoretical works [4,6] concerning  $^{91}\text{Zr}$  were developed within the framework of the shell model, and newly available data presented in Ref. [12], especially on electromagnetic properties, were not analyzed.

The formalism of the cluster-phonon model is developed in Sec. II. In order to test the parametrization of the residual proton-proton and proton-neutron interactions and other parameters, the same coupling model, with the adequate cluster configurations, was applied to the description of the  $^{90}\text{Zr}$  and  $^{90}\text{Y}$  spectra. The final set of parameters is presented in Sec. III. The results obtained are discussed and compared with experiment in Sec. IV. Finally, the conclusions are drawn in Sec. V.

### II. THE NUCLEAR MODEL

A detailed description of the cluster vibrator model is given in Refs. [13,14]. Here we only sketch the main formulas in order to establish the notation. The total Ham-

iltonian is

$$H = H_0 + H_{\text{res}} + H_{\text{int}}, \quad (1)$$

where  $H_0$  represents the energy of the unperturbed system consisting of quadrupole and octupole vibrational fields and valence particles in a central field. The effective proton-proton and proton-neutron residual interactions among the particles in the shell-model cluster,  $H_{\text{res}}$ , only include explicitly the modified surface  $\delta$  interaction (MSDI). This two-body force is expressed in the form [15]

$$H_{\text{res}} = -4\pi A_T \delta(\mathbf{r}(1) - \mathbf{r}(2)) \delta(r(1) - R_0) + B[\boldsymbol{\tau}(1) \cdot \boldsymbol{\tau}(2)], \quad (2)$$

where  $\mathbf{r}$  and  $\boldsymbol{\tau}$  are the position and isospin vector operators of the interacting particles and  $R_0$  the nuclear radius. The isospin  $T$  is used to label the strength parameters  $A_1$  and  $A_0$  for  $T=1$  and  $0$ , respectively. The last term contributes only to the diagonal matrix elements, and is necessary only for  $^{91}\text{Zr}$  calculations. The interaction between the  $p$ -particle cluster and the vibrational fields is given by the expression [16]

$$H_{\text{int}} = \sum_{\lambda=2}^3 \frac{\beta_\lambda}{(2\lambda+1)^{1/2}} \times \sum_{\mu=-\lambda}^{\lambda} [b_\lambda^{\mu+} + (-)^{\lambda-\mu} b_\lambda^{-\mu}] \times \sum_{i=1}^p k(r_i) Y_{\lambda\mu}^*(\theta_i, \phi_i), \quad (3)$$

where  $k(r_i)$  is the interaction intensity,  $\beta_\lambda$  are the deformation parameters, and all other symbols have the standard meaning.

The matrix elements of  $H_{\text{int}}$  are parametrized by the coupling constants  $a_\lambda$  defined

$$a_\lambda = \frac{\langle k \rangle}{\sqrt{4\pi}} \frac{\beta_\lambda}{\sqrt{2\lambda+1}}, \quad (4)$$

where  $\langle k \rangle$  is the mean value of the radial matrix element of the interaction.

The eigenvalue problem (1) is solved in the basis

$$|(j_1 j_2) J_{12}, R; I\rangle$$

for the  $A=90$  nuclei ( $p=2$ ) and in the basis

$$|(j_1 j_2) J_{12, j_3} | J, R; I\rangle$$

for the  $A=91$  nucleus ( $p=3$ ). Here  $j=(nj)$  stands for the quantum numbers of the single proton or neutron state,  $J$  stands for the total angular momentum of the cluster,  $R$  represent the quantum numbers  $\{N_2 R_2, N_3 R_3, R\}$ , where  $N_\lambda$  is the number of  $\lambda$ -pole phonons of angular momentum  $R_\lambda$ ,  $\mathbf{R} = \mathbf{R}_2 + \mathbf{R}_3$ , and  $I$  is the total angular momentum.

The electric and magnetic operators consist of a particle and a collective part:

$$\begin{aligned} \mathcal{M}(E\lambda, \mu) &= \sum_{i=1}^p e^{\text{eff}}(i) r^\lambda(i) Y_{\lambda\mu}(\theta_i, \phi_i) \\ &\quad + \frac{3}{4\pi} e_v^{\text{eff}} R_0^\lambda [b_\lambda^{\mu+} + (-)^{\mu-\lambda} b_\lambda^{-\mu}], \quad (5) \\ \mathcal{M}(M1, \mu) &= \left[ \frac{3}{4\pi} \right]^{1/2} \left[ g_R R_\mu \right. \\ &\quad \left. + \sum_{i=1}^p [g_s(i) S_\mu(i) \right. \\ &\quad \left. + g_l(i) L_\mu(i)] \right] \mu_N, \quad (6) \end{aligned}$$

where  $e_p^{\text{eff}}$  is the effective particle charge,  $e_v^{\text{eff}} = Ze\beta_\lambda / \sqrt{2\lambda+1}$  is the effective vibrator charge, and  $g_R$ ,  $g_l$ , and  $g_s$  are, respectively, the collective, orbital, and spin gyromagnetic ratios.

The mixing ratio  $\delta(E2/M1)$  is given by

$$\delta(E2/M1) = 0.835 (E_\lambda / \text{MeV}) (\mathcal{D} / eb\mu_N^{-1}) \quad (7)$$

with

$$\mathcal{D} = \frac{\langle I_i || \mathcal{M}(E2) || I_f \rangle}{\langle I_i || \mathcal{M}(M1) || I_f \rangle}, \quad (8)$$

and  $E_\gamma = E_i - E_f$  is the transition energy.

The reduced transition probabilities are

$$B(\bar{\omega}L; I_i \rightarrow I_f) = \frac{\langle I_i || \mathcal{M}(\bar{\omega}L) || I_f \rangle^2}{2J_i + 1} \quad (9)$$

with  $\bar{\omega}L = E2, M1$  for electric and magnetic cases, respectively. The matrix elements of  $E2$  and  $M1$  operators are expressed in the forms

$$\langle I_i || \mathcal{M}(E\lambda) || I_f \rangle = (e_p^{\text{eff}} A + e_n^{\text{eff}} A' + e_v^{\text{eff}} B) e \text{ fm}^\lambda, \quad (10a)$$

$$\langle I_i || \mathcal{M}(1) || I_f \rangle = (g_s^{\text{eff}} C + g_n^{\text{eff}} C' + g_l^{\text{eff}} D + g_l^{\text{eff}} D' + g_R E) \mu_N, \quad (10b)$$

and the quantities  $A$ ,  $A'$ ,  $B$ ,  $C$ ,  $C'$ ,  $D$ ,  $D'$ , and  $E$  are calculated from the model wave functions.

### III. PARAMETERS

The cluster is assumed to consist of two single protons and one single neutron distributed among the single proton states:  $2p_{1/2}$  and  $1g_{9/2}$ , and the single neutron states  $2d_{5/2}$ ,  $3s_{1/2}$ ,  $2d_{3/2}$ ,  $2g_{7/2}$ , and  $1h_{11/2}$ , and coupled to  $N=0, 1, 2$  quadrupole phonon and  $N=0, 1$  octupole phonon.

The Hamiltonian was diagonalized with the following set of parameters.

(a) Single-particle energies  $\varepsilon_{p_{1/2}} = 0$ ,  $\varepsilon_{g_{9/2}} = 1.00$  MeV,  $\varepsilon_{d_{5/2}} = 0$ ,  $\varepsilon_{s_{1/2}} = 1.08$  MeV,  $\varepsilon_{d_{3/2}} = 2.26$  MeV,  $\varepsilon_{g_{7/2}} = 2.34$  MeV, and  $\varepsilon_{h_{11/2}} = 2.73$  MeV, based on the values employed in Refs. [4,11].

(b) Phonon energies  $\hbar\omega_2 = 1.836$  MeV and  $\hbar\omega_3 = 2.734$  MeV are the experimental energies of  $2_1^+$  and  $3_1^-$  states in the  $^{88}\text{Sr}$  nucleus.

(c) MSDI strengths  $A_0=0.4$  MeV,  $A_1=0.4$  MeV, and  $B=0.73$  MeV.

(d) Particle-vibration coupling constants  $a_2=0.41$  MeV and  $a_3=0.63$  MeV were obtained using the deformation parameters  $\beta_2=0.110$  and  $\beta_3=0.196$ , that reproduce the  $B(E2)$  and  $B(E3)$  experimental data [17], and the fixed value  $\langle K \rangle=30$  MeV taken from Ref. [11]. This value for  $\beta_2$  is equal to the measured value [18], and for  $\beta_3$  is a little greater than the experimental data ( $\beta_3=0.178\pm 0.009$ ) [19].

The electromagnetic properties were obtained with the usual values of the effective electric charge and effective gyromagnetic ratios: namely,

$$\left. \begin{array}{l} \text{set I: } e_n^{\text{eff}}=0.5e \\ \text{set II: } e_n^{\text{eff}}=1.0e \\ \text{set III: } e_n^{\text{eff}}=1.5e \end{array} \right\}, e_v^{\text{eff}}=\frac{Ze\beta_\lambda}{\sqrt{2\lambda+1}}, e_p^{\text{eff}}=2.0e$$

for the electric transitions, and

$$\left. \begin{array}{l} \text{set I: } g_{sp}^{\text{eff}}=g_{sp}^{\text{free}}, g_{sn}^{\text{eff}}=g_{sn}^{\text{free}} \\ \text{set II: } g_{sp}^{\text{eff}}=0.7g_{sp}^{\text{free}}, g_{sn}^{\text{eff}}=0.7g_{sn}^{\text{free}} \\ \text{set III: } g_{sp}^{\text{eff}}=0.5g_{sp}^{\text{free}}, g_{sn}^{\text{eff}}=0.5g_{sn}^{\text{free}} \end{array} \right\}, g_{l_p}=1, g_{l_n}=0, g_R=0$$

for the magnetic ones.

In the calculations of electric properties we used for the radial matrix elements  $\langle j_a | r^\lambda | j_b \rangle$  the usual estimate  $\langle r^\lambda \rangle = [3/(\lambda+3)]R_0^\lambda$  with a nuclear radius  $R_0=1.20A^{1/3}$ .

IV. RESULTS AND DISCUSSION

A.  $^{90}\text{Zr}$  and  $^{90}\text{Y}$

The goal of the present calculations for these nuclei is to test the parametrization quoted in the previous section. The calculations were performed within the frame-

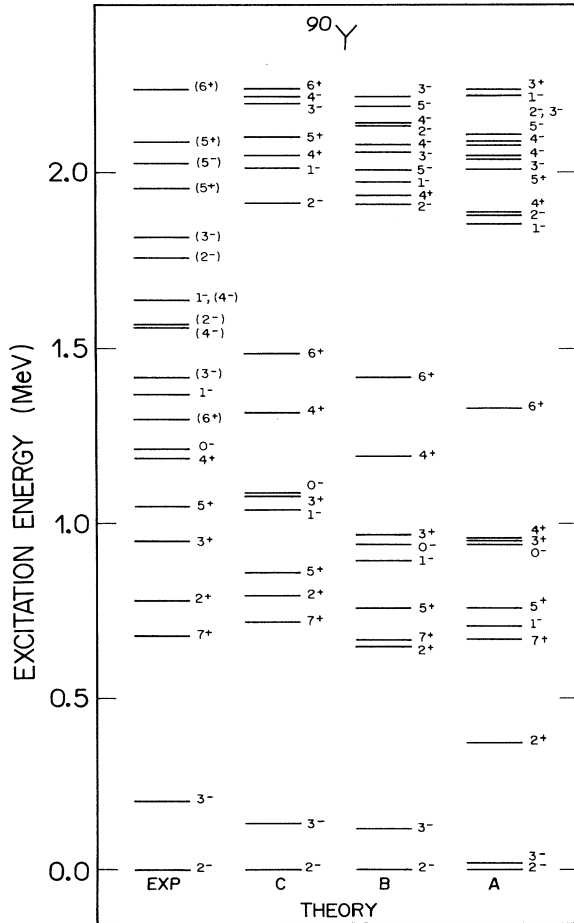


FIG. 1. Comparison of experimental levels of  $^{90}\text{Y}$  from Ref. [20] with the calculated spectra.

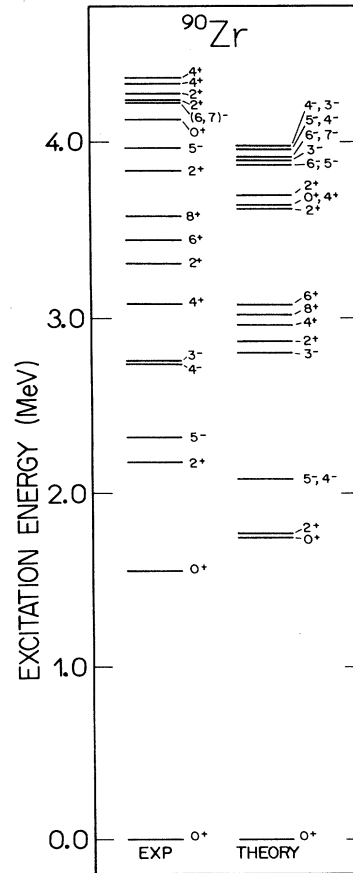


FIG. 2. Comparison of experimental levels of  $^{90}\text{Zr}$  from Ref. [20] with the calculated spectra.

work of the model and parameters presented in earlier sections with the following cluster configurations. For  $^{90}\text{Zr}$  and  $^{90}\text{Y}$  these are constituted, respectively, by coupled two single proton and one single proton plus one single neutron distributed on the corresponding single-particle states.

The experimental [20] and theoretical spectra for  $^{90}\text{Y}$  are compared in Fig. 1. In the last column (theory A) the results displayed were obtained with the same parametrization used for  $^{91}\text{Zr}$ . It should be noted that better agreement between the calculated and measured energy spectra can be improved by lowering the MSDI strength to  $A_1=0.20$  MeV (theory B) and increasing the octupolar coupling parameter to  $a_3=0.84$  MeV (theory C), which corresponds to take  $\langle K \rangle=40$  MeV with settled  $\beta_3$ . Usually, the particle-vibration coupling intensities have been used as an adjustable parameter. For this mass region they correspond to the  $\langle K \rangle$  values in the range 20–40 MeV [5,10,11]. The change on the parameter  $A_1$  is analyzed after the discussion of  $^{90}\text{Zr}$  results performed below. Although the single proton space is restricted to  $p_{1/2}$  and  $g_{9/2}$  states, particularly for positive-parity levels, there is good agreement. In the case of negative-parity states, only the first  $2^-$ ,  $3^-$ ,  $1^-$ , and  $0^-$  levels can be described by this model proton space, as all the other levels below 2 MeV are dominated by configurations that include the single proton  $p_{3/2}$  and  $f_{5/2}$  orbitals [21].

In Fig. 2, the spectra for  $^{90}\text{Zr}$ , experimental [20] and that obtained with the parametrization of Sec. III

(theory), are compared. It was verified by means of an extended shell-model calculation [9] that, for the states  $0_1^+$ ,  $0_2^+$ ,  $4_1^+$ ,  $2_2^+$ ,  $6_1^+$ , and  $8_1^+$  the core-excited configuration, for two holes in the  $p_{3/2}$  and  $f_{5/2}$  orbitals, ranges from 30 to 45%, the first  $5^-$  and  $4^-$  are members of the doublet with configuration  $(p_{1/2}g_{9/2})$  and the others,  $5^-$ ,  $6^-$ , and  $7^-$ , up to 4.6 MeV have the principal configuration  $(f_{5/2}^{-1}g_{9/2})$  or  $(p_{3/2}^{-1}g_{9/2})$ . The agreement between experiment and theory, within the restricted  $(p_{1/2}, g_{9/2})$  proton space, is reasonable.

The need of different values for the MSDI parameter  $A_1$  to adjust  $^{90}\text{Zr}$  and  $^{90}\text{Y}$  spectra is expected once that the effective proton-proton and proton-neutron residual interactions occur in unlike shells. In this mass region, without core excitation, Chuu *et al.* [4] employed for the effective proton-neutron interaction in  $(p_{1/2}, g_{9/2})$  and  $(d_{5/2}, s_{1/2}, d_{3/2}, g_{9/2})$  space a SDI force with  $A_0=0.45$  MeV and  $A_1=0.09$  MeV, and fitted matrix elements for proton-proton interaction in  $(p_{1/2}, g_{9/2})$  space which are numerically similar those derived from a SDI force with  $A_1=0.40$  MeV.

In the  $^{91}\text{Zr}$  calculations presented in the following, we have considered the same two-body force for proton-proton and proton-neutron residual interactions. Therefore, in the case of  $T=1$  matrix elements there are mixed proton-proton and proton-neutron contributions. The final fit shows that the proton-proton interaction intensities are predominant.

### B. $^{91}\text{Zr}$

The calculated energy spectra for positive- and negative-parity levels is compared with experiment [12] in Fig. 3. In the case of positive-parity states, the calculations reproduce the experimental sequence for the first six levels. The number of levels predicted for each spin is in near agreement with the experiment, and, in agreement with experimental data, one state of  $\frac{21}{2}^+$  and one of  $\frac{17}{2}^+$  should exist near 3.0 MeV of excitation energy.

In the case of negative-parity states, the number of levels calculated up to 3.2 MeV is smaller than measured. This suggests that for negative-parity low-lying levels the influence of core excitations, such as particle-hole excitations involving  $f_{5/2}$  and  $p_{3/2}$  proton orbitals, is more pronounced than for positive-parity ones.

The configurations and amplitudes of the wave functions of low-lying states which contribute more than 9% are listed in Table I. The first positive-parity states have a mixed three-particle and one quadrupole-phonon characteristic. Only  $\frac{5}{2}^+$  and  $\frac{7}{2}^+$  are composed of pure three-particle configurations. The first negative-parity  $\frac{3}{2}^-$ ,  $\frac{5}{2}^-$ ,  $\frac{7}{2}^-$ , and  $\frac{9}{2}^-$  states are pure three-particle states. For the  $\frac{11}{2}^-$  and  $\frac{13}{2}^-$  states there are mixtures of one-octupole-phonon components and for  $\frac{13}{2}^-$  and  $\frac{15}{2}^-$  one-quadrupole phonon components.

Experimental data on the electromagnetic properties [12] are compared with the calculated values in Table II. In general, the measured values can be reproduced by theoretical calculations adjusting the effective neutron charge and effective gyromagnetic ratios for electric and

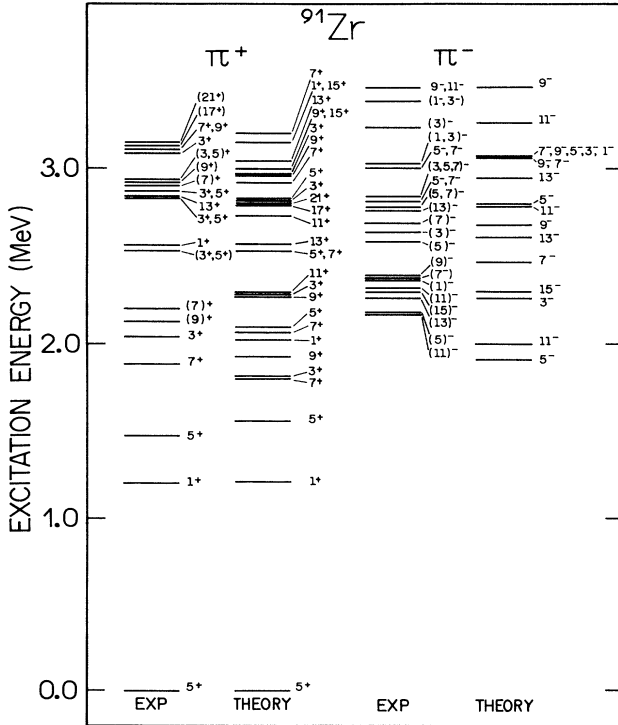


FIG. 3. Comparison of experimental levels of  $^{91}\text{Zr}$  from Ref. [12] with the calculated spectra.

magnetic observables, respectively. All signs and magnitudes of the electromagnetic moments are in agreement with experiment, and the theory reinforces the attribution of a negative quadrupole moment for the first  $\frac{21}{2}^+$  state. The measured magnitudes of the  $B(E2)$  rates are reproduced, except for the  $\frac{3}{2}^+ \rightarrow \frac{5}{2}^+$  transition. The ex-

TABLE I. Wave functions of low-lying states in  $^{91}\text{Zr}$ . Only those amplitudes which are larger than 9% are listed.

$I_i^\pi$	$j_a$	$j_b$	$j_{ab}$	$j_c$	$J$	$N$	$R$	Amplitude
$\frac{1}{2}^+$	$\frac{9}{2}$	$\frac{9}{2}$	0	$\frac{1}{2}$	$\frac{1}{2}$	0	0	0.709
	$\frac{9}{2}$	$\frac{9}{2}$	2	$\frac{5}{2}$	$\frac{1}{2}$	0	0	-0.307
	$\frac{1}{2}$	$\frac{1}{2}$	0	$\frac{1}{2}$	$\frac{1}{2}$	0	0	-0.305
	$\frac{1}{2}$	$\frac{1}{2}$	0	$\frac{5}{2}$	$\frac{5}{2}$	1	2	0.306
$\frac{3}{2}^+$	$\frac{9}{2}$	$\frac{9}{2}$	0	$\frac{3}{2}$	$\frac{3}{2}$	0	0	-0.312
	$\frac{1}{2}$	$\frac{1}{2}$	0	$\frac{3}{2}$	$\frac{3}{2}$	0	0	0.462
	$\frac{9}{2}$	$\frac{9}{2}$	0	$\frac{5}{2}$	$\frac{5}{2}$	1	2	-0.446
	$\frac{1}{2}$	$\frac{1}{2}$	0	$\frac{5}{2}$	$\frac{5}{2}$	1	2	0.421
$\frac{5}{2}^+$	$\frac{9}{2}$	$\frac{9}{2}$	0	$\frac{5}{2}$	$\frac{5}{2}$	0	0	-0.466
	$\frac{1}{2}$	$\frac{1}{2}$	0	$\frac{5}{2}$	$\frac{5}{2}$	1	2	-0.655
	$\frac{1}{2}$	$\frac{1}{2}$	0	$\frac{5}{2}$	$\frac{5}{2}$	0	0	0.671
	$\frac{1}{2}$	$\frac{1}{2}$	0	$\frac{5}{2}$	$\frac{5}{2}$	0	0	0.646
$\frac{5}{2}^+$	$\frac{9}{2}$	$\frac{9}{2}$	0	$\frac{5}{2}$	$\frac{5}{2}$	0	0	0.461
	$\frac{9}{2}$	$\frac{9}{2}$	2	$\frac{5}{2}$	$\frac{5}{2}$	0	0	0.457
	$\frac{9}{2}$	$\frac{9}{2}$	2	$\frac{5}{2}$	$\frac{5}{2}$	0	0	0.614
	$\frac{9}{2}$	$\frac{9}{2}$	4	$\frac{5}{2}$	$\frac{7}{2}$	0	0	0.360
$\frac{7}{2}^+$	$\frac{9}{2}$	$\frac{9}{2}$	0	$\frac{5}{2}$	$\frac{5}{2}$	1	2	0.445
	$\frac{1}{2}$	$\frac{1}{2}$	0	$\frac{5}{2}$	$\frac{5}{2}$	1	2	-0.385
	$\frac{9}{2}$	$\frac{9}{2}$	2	$\frac{5}{2}$	$\frac{9}{2}$	0	0	0.462
	$\frac{9}{2}$	$\frac{9}{2}$	4	$\frac{5}{2}$	$\frac{9}{2}$	0	0	0.300
$\frac{9}{2}^+$	$\frac{9}{2}$	$\frac{9}{2}$	0	$\frac{5}{2}$	$\frac{5}{2}$	1	2	-0.517
	$\frac{1}{2}$	$\frac{1}{2}$	0	$\frac{5}{2}$	$\frac{5}{2}$	1	2	0.528
	$\frac{1}{2}$	$\frac{9}{2}$	4	$\frac{5}{2}$	$\frac{9}{2}$	0	0	0.927
	$\frac{1}{2}$	$\frac{9}{2}$	5	$\frac{5}{2}$	$\frac{9}{2}$	0	0	0.914
$\frac{7}{2}^-$	$\frac{1}{2}$	$\frac{9}{2}$	5	$\frac{5}{2}$	$\frac{7}{2}$	0	0	0.881
	$\frac{1}{2}$	$\frac{9}{2}$	5	$\frac{5}{2}$	$\frac{9}{2}$	0	0	0.918
	$\frac{1}{2}$	$\frac{1}{2}$	0	$\frac{11}{2}$	$\frac{11}{2}$	0	0	-0.532
	$\frac{9}{2}$	$\frac{9}{2}$	0	$\frac{11}{2}$	$\frac{11}{2}$	0	0	0.422
$\frac{11}{2}^-$	$\frac{1}{2}$	$\frac{9}{2}$	5	$\frac{5}{2}$	$\frac{11}{2}$	0	0	0.455
	$\frac{1}{2}$	$\frac{1}{2}$	0	$\frac{5}{2}$	$\frac{5}{2}$	1	3	-0.382
	$\frac{9}{2}$	$\frac{9}{2}$	0	$\frac{5}{2}$	$\frac{5}{2}$	1	3	0.316
	$\frac{1}{2}$	$\frac{9}{2}$	5	$\frac{5}{2}$	$\frac{11}{2}$	0	0	0.797
$\frac{13}{2}^-$	$\frac{1}{2}$	$\frac{1}{2}$	0	$\frac{5}{2}$	$\frac{5}{2}$	1	3	0.371
	$\frac{9}{2}$	$\frac{9}{2}$	0	$\frac{5}{2}$	$\frac{5}{2}$	1	3	-0.337
	$\frac{1}{2}$	$\frac{9}{2}$	4	$\frac{5}{2}$	$\frac{13}{2}$	0	0	0.843
	$\frac{1}{2}$	$\frac{9}{2}$	5	$\frac{5}{2}$	$\frac{13}{2}$	0	0	0.376
$\frac{15}{2}^-$	$\frac{1}{2}$	$\frac{9}{2}$	4	$\frac{5}{2}$	$\frac{13}{2}$	1	2	-0.307
	$\frac{1}{2}$	$\frac{9}{2}$	5	$\frac{5}{2}$	$\frac{15}{2}$	0	0	0.926
	$\frac{1}{2}$	$\frac{9}{2}$	5	$\frac{5}{2}$	$\frac{15}{2}$	1	2	-0.335
	$\frac{1}{2}$	$\frac{9}{2}$	5	$\frac{5}{2}$	$\frac{15}{2}$	1	2	-0.335

TABLE II. Comparison between experiment and theory. The magnitude dipole and electric quadrupole moments are in units of  $\mu_N$  and  $e b$ , respectively. The  $B(M1)$  and  $B(E2)$  values are both in W.u. Theories I, II, and III refer, respectively, to sets I, II, and III presented in Sec. III.

Quantity	Experiment		Theory			
			I	II	III	
$\mu_{5/2_1^+}$	-1.303	62	2	-1.73	-1.19	-0.82
$Q_{5/2_1^+}$	-0.206	10		-0.197	-0.251	-0.304
$\mu_{15/2_1^-}$	+5.25	8		+4.61	+4.62	+4.63
$\mu_{21/2_1^+}$	+9.82	8		+10.12	+9.21	+8.60
$Q_{21/2_1^+}$	(- )0.86	5		-0.65	-0.71	-0.77
$B(M1)$						
$\frac{5}{2}^+ \rightarrow \frac{5}{2}^+$	0.037 <sup>a</sup>	18		0.014	0.009	0.007
$\frac{7}{2}^+ \rightarrow \frac{5}{2}^+$	0.022	+10-19		0.036	0.024	0.017
$\frac{3}{2}^+ \rightarrow \frac{5}{2}^+$	0.23 <sup>a</sup>	2		0.22	0.44	0.79
$\frac{7}{2}^+ \rightarrow \frac{5}{2}^+$	0.0008	26		0.0016	0.0016	0.0015
$\frac{15}{2}^- \rightarrow \frac{13}{2}^-$	0.0346	13		0.0058	0.0007	0.0089
$B(E2)$						
$\frac{1}{2}^+ \rightarrow \frac{5}{2}^+$	54	19		0.10	28	76
$\frac{5}{2}^+ \rightarrow \frac{5}{2}^+$	18 <sup>b</sup>	9		1.4	44	41
$\frac{7}{2}^+ \rightarrow \frac{5}{2}^+$	6	+6-3		6.6	7.0	7.4
$\frac{3}{2}^+ \rightarrow \frac{5}{2}^+$	60 <sup>b</sup>	5		2.9	3.4	4.0
$\frac{9}{2}^+ \rightarrow \frac{5}{2}^+$	4.4	7		5.7	6.0	6.3
$\frac{7}{2}^+ \rightarrow \frac{5}{2}^+$	0.9	5		0.6	0.3	0.5
$\frac{21}{2}^+ \rightarrow \frac{17}{2}^+$	4.10	21		2.39	3.14	4.00

<sup>a</sup>Upper limit for  $B(E2)=0$ .

<sup>b</sup>Upper limit for  $B(M1)=0$ .

perimental magnitudes of the  $B(M1)$  rates for the  $\frac{7}{2}^+ \rightarrow \frac{5}{2}^+$  and  $\frac{3}{2}^+ \rightarrow \frac{5}{2}^+$  transitions are reproduced and the others, except for the  $\frac{15}{2}^- \rightarrow \frac{13}{2}^-$  transition, are near the lower experimental limit.

## V. CONCLUSIONS

We have demonstrated that the properties of the  $^{91}\text{Zr}$  nucleus arise from a two-proton-one-neutron cluster core coupling model, where the cluster of particles is coupled to the quadrupole and octupole vibration fields of the  $^{88}\text{Sr}$  core. Within this picture the available data on the energy spectrum, electric and magnetic moments, and  $B(E2)$  and  $B(M1)$  values were examined. This simple model can be considered as a good starting point for further theoretical calculations. The core correlations not included due to the particle-hole proton excitations may affect in an appreciable way only the properties of the low-energy negative-parity levels.

## ACKNOWLEDGMENTS

We would like to thank F. Krmpotić for fruitful discussions and W. A. Seale for a critical reading of the manuscript. This work was supported in part by

Fundação de Amparo à Pesquisa do Estado de São Paulo (FAPESP), Conselho Nacional de Desenvolvimento Científico e Tecnológico (CNPq), and Coordenação de Aperfeiçoamento de Pessoal do Ensino Superior (CAPES).

- 
- [1] I. Talmi, *Phys. Rev.* **126**, 2116 (1962).  
 [2] D. H. Gloeckner, *Nucl. Phys.* **A253**, 301 (1975).  
 [3] S. S. Ipson, K. C. McLean, W. Booth, J. G. B. Haigh, and R. N. Glover, *Nucl. Phys.* **A253**, 189 (1975).  
 [4] D. S. Chuu, M. M. King Yen, Y. Sham, and S. T. Hsieh, *Nucl. Phys.* **A321**, 415 (1979).  
 [5] Th. Paradellis, S. Hontzeas, and H. Blok, *Nucl. Phys.* **A168**, 539 (1971).  
 [6] R. M. Anazawa, M. N. Rao, W. A. Seale, R. V. Ribas, H. Dias, and L. Losano, *Rev. Bras. Fis.* **20**, 68 (1990).  
 [7] O. Schwentker, J. Dawson, S. McCaffrey, J. Robb, J. Heisenberg, J. Lichtenstadt, C. N. Papanicolas, J. Wise, J. S. McCarthy, N. Hintz, and H. P. Blok, *Phys. Lett.* **112B**, 40 (1982).  
 [8] J. Heisenberg, J. Dawson, T. Milliman, O. Schwentker, J. Lichtenstadt, C. N. Papanicolas, J. Wise, J. S. McCarthy, N. Hintz, and H. P. Block, *Phys. Rev. C* **29**, 97 (1984).  
 [9] Xiangdong Ji and B. H. Wildenthal, *Phys. Rev. C* **37**, 1256 (1987).  
 [10] C. A. Heras and S. M. Abecasis, *Phys. Rev. C* **27**, 1765 (1983).  
 [11] C. A. Heras and S. M. Abecasis, *Z. Phys. A* **324**, 403 (1986).  
 [12] H. W. Müller, *Nucl. Data Sheets* **60**, 835 (1990).  
 [13] G. Alaga, in *Nuclear Structure and Nuclear Reactions*, Proceedings of the International School of Physics, "Enrico Fermi," Course XI, edited by M. Jean and R. A. Ricci (Academic, New York, 1969).  
 [14] V. Paar, *Heavy-Ion, High-Spin States and Nuclear Structure* (IAEA, Vienna, 1975), Vol. II, p. 179.  
 [15] B. J. Brusaard and P. W. M. Glaudemans, *Shell Model Applications in Nuclear Spectroscopy* (North-Holland, Amsterdam, 1977).  
 [16] A. Bohr and B. Mottelson, *Nuclear Structure* (Benjamin, New York, 1975).  
 [17] L. T. van der Bijl, H. P. Blok, R. Frey, D. Meuer, A. Richter, and P. K. A. de Witt Huberts, *Z. Phys. A* **305**, 231 (1982); L. T. van der Bijl, H. Blok, H. P. Blok, R. Ent, J. Heisenberg, O. Schwentker, A. Richter, and P. K. A. de Witt Huberts, *J. Phys. (Paris)* **45**, C4-465 (1984).  
 [18] F. T. Baker, S. Davis, C. Glashauser, and A. B. Robbins, *Nucl. Phys.* **A250**, 79 (1975); O. Hansen, F. Videback, E. R. Flynn, J. C. Peng, and J. A. Cizewski, *ibid.* **A364**, 144 (1981).  
 [19] R. W. Finlay, M. H. Hadizadeh, J. Rapaport, and D. E. Bainum, *Nucl. Phys.* **A344**, 257 (1980).  
 [20] D. C. Kocher, *Nuclear Data Sheets* **16**, 55 (1975); in *Table of Isotopes*, edited by C. M. Lederer and V. S. Shirley (Wiley, New York, 1978).  
 [21] D. J. Decman and R. K. Sheline, *Z. Phys. A* **312**, 209 (1983).